Progress and perspectives on strategies to control photochemical properties in Metallo-Dithiolene Donor-Acceptor systems

Inorganica Chimica Acta xxx (xxxx) 120731

Contents lists available at ScienceDirect

Inorganica Chimica Acta

journal homepage: www.elsevier.com/locate/ica

Progress and perspectives on strategies to control photochemical properties in Metallo-Dithiolene Donor-Acceptor systems

Flavia Artizzu [a,*], Davide Espa [b], Luciano Marchiò [c], Luca Pilia [b,*], Angela Serpe [d], Paola Deplano [d,*]

[a] Dipartimento di Scienze e Innovazione Tecnologica, Università del Piemonte Orientale, viale Teresa Michel 11, 15121 Alessandria Italy
[b] Dipartimento di Ingegneria Meccanica, Chimica e dei Materiali, Università di Cagliari, Via Marengo 2, 09123 Cagliari Italy
[c] Dipartimento SCVSA, Università di Parma, Parco Area delle Scienze 17/a, 43124 Parma, Italy
[d] Dipartimento di Ingegneria Civile, Ambientale e Architettura, INSTM Research Unit, Università di Cagliari, Via Marengo 2, 09123 Cagliari, Italy

ARTICLE INFO

Keywords:
Donor acceptor systems
D^8-metals
Dithiolenes
Quadratic hyperpolarizability
Fluorescence
Optical switches

ABSTRACT

In this mini-review recent progress in studies on heteroleptic d^8-metal dithiolene complexes with a D-M-A donor–π–acceptor electronic structure showing non-linear and linear optical properties, are presented. The ligands, formally dithiolenes, consist in a variety of donors (dithiolato) and acceptors (dithioxamide and dithioxamidate), differing for electronic properties and/or structural features, varying from rigid and planar systems to conformationally-flexible ones. It is shown how the components of these D-M-A systems modulate both the energy and topology of the frontier molecular orbitals involved in the charge transport mechanism to reach a fine tuning of the optical properties and achieve high values of the quadratic hyperpolarizability. Further tailoring of the ligands by integrating specific functional groups in their periphery, such as NH and/or a quinoxaline ring, is presented as a versatile tool to achieve a reversible response to external stimuli. Accordingly, selected cases where exchange color proton and silver ions tunable properties, switching of the NLO-response (with a 2.5–6.5 contrast for HCl exchange) and also uncommon emission color reversibly tunable by different stimuli, such as proton and silver ions, are presented. In the bulk, crystals gave a poor or null SHG response, while a stable and large response has been obtained in a limited number of cases of complexes dispersed in PMMA films. Reported results are addressed to stimulate further work to exploit the potential of this class of complexes as molecular sensors and switches and to optimize the processing procedures to achieve good SHG responses in the bulk.

1. Introduction

Donor–acceptor conjugated molecules (D-π-A) represent a versatile class of compounds that, due to their inherent low-energy intramolecular charge-transfer (ICT) band in the visible to the near infrared (NIR) region, are of interest as building blocks for advanced photonic materials. In particular they can work as second-order nonlinear optical (NLO) chromophores. Second-order NLO effects arise from the first hyperpolarizability β, which at the molecular level relates to the way in which the mobile electronic charges respond to the oscillating electric field of a laser beam [1]. To observe quadratic NLO effects in the bulk, a polar ordering of the NLO chromophore, resulting in a second harmonic generation (SHG), is required and different strategies can be employed to achieve this goal [2]. A versatile one comprises the formation of poled polymers, where the required asymmetry is imposed by the external electric field, while heating [3]. Among other strategies, the introduction of chiral groups in the molecules represents a chance to obtain crystals in a suitable non-centrosymmetric space group [4].

Several organic D-π-A molecules have been and still are extensively investigated as 2nd NLO-phores [5–10]. In addition suitable transition metal complexes, where the metal works as a π-bridge between the Donor and the Acceptor ligands, play an important role in this field because they can provide improved stability for ligands and suitable-metals can favor co-planarity through their preferred coordination geometry, maximizing the CT Donor-Acceptor transition [11]. Moreover the opportunity to properly engineering the organic ligands, can favor the incorporation of the metal-complexes into suitable polymeric matrices and allows expanding their properties by integrating specific functional groups capable to respond to external stimuli (protons, metal ions, light-irradiation) [12]. Among these, several classes of d^8-metal complexes where the metal is coordinated to a variety of ligands spanning from nitrogen ligands, cyclometalated, alkynyl to sulfur ligands [13, −21]. An updating on these systems addressed to highlight the spe-

* Corresponding authors.
E-mail addresses: flavia.artizzu@uniupo.it (F. Artizzu), pilialuc@unica.it (L. Pilia), deplano@unica.it (P. Deplano).

https://doi.org/10.1016/j.ica.2021.120731
Received 1 October 2021; Received in revised form 26 November 2021; Accepted 26 November 2021
0020-1693/

cial role of related platinum complexes as NLO-active chromophores and their potential for electrooptical devices and optical communications, can be found in a recent interesting review by V. Guerchais, D. Roberto *et al.* [22]. In D-M-A complexes an asymmetric charge distribution can also be reached where both ligands can be formally taken as dithiolene ligands. As known, dithiolene ligands are capable to undergo reversible redox processes, which involve the filling of the four frontier orbitals (FOs) of π-symmetry (the first two occupied in dithioketone, the third in ene-1,2-dithiolate) as shown in Scheme 1 [23,24].

It is well established that the nature of R-substituents affects the energy of these FOs, which are pushed up or down by electron-donating or electron-withdrawing groups respectively, thus stabilizing the dithione or the dithiolate form. Accordingly, the tuning of substituents in heteroleptic dithiolenes where a π-donor (D, the dithiolato) and a π-acceptor (A, the dithione) ligand are connected by a d^8-metal in a square-planar coordination, allows one to obtain low-energy-gap molecules where the metal acts as a suitable π-bridge for the D-A intramolecular charge transfer (ICT) transition. The ICT D–A process produces a decrease of the dipole moment from the ground to the excited state and, as a consequence, a negative solvatochromism and first hyperpolarizability (β) are predictable, in agreement with the two-state theoretical approximation, which takes into account a single excited state for the dependence of the hyperpolarizability tensor element oriented along the dipolar axis. Accordingly β is directly proportional to $\Delta\mu_{eg}$ (the difference in dipole moment between the lowest unoccupied, LUMO, and the highest occupied, HOMO, molecular orbital), to the square of the transition dipole moment μ_{ge} (oscillator strength) and inversely proportional to the square of ΔE_{ge}, the energy difference between ground and CT excited states [25,26]. When the electron density is symmetrically distributed along the molecular long axis, $\Delta\mu_{eg} \approx 0$ and β will disappear. This approximation provides useful guidelines to synthetic chemists for properly design the components of a D-M-A system. Thus, the CT in these systems controls both the linear and the nonlinear optical properties and can be readily modulated by a proper selection of the ligands, which affect the FOs, as pictorially summarized in Fig. 1.

$$\beta \propto \frac{\Delta\mu_{eg}(\mu_{ge})^2}{\Delta E_{ge}^2}$$

In Chart 1 the molecular structures and names of Donor and Acceptor ligands mentioned in this paper are listed. As far as the Donors are concerned, they differ either for the electron-accepting capability of the substituents at the C2S2 moieties (similar in **D_1**-**D_2**-**D_3**; and increasing from **D_3** to **D_6**) ligand, and/or for the structural features varying from rigid and planar systems (**D_1**, **D_5**); to terminal groups connected through a thio-ether bridge (**D_2** and **D_3**) or conformationally flexible ester groups (**D_4**).

The acceptors bear NR groups as electron-donating substituents at the C2S2 moiety. The acyclic dithio-oxamidate (**A_1**) [(*R*)-*α*-MBAdtox] contains the homochiral stereo-center *R* = (+) α-methylbenzyl and can form a tight-ion paired species with HCl (**A_1·HCl**), and the cyclic dithioxamide R_2pipdt (**A_2**) where the NR frames are inserted in a *hexa*-atomic ring. The accepting capability of these ligands follows the order **A_1** < **A_1·HCl** < **A_2**. The class of dithio-oxamidate ligands and the properties of related metal complexes have been and still are object of an extensive investigation by Campagna, Lanza and co-workers. It has been found that platinum homoleptic complexes coordinated to N,N′-dialkyldithio-oxamidate are capable to work as HCl transporters across a hydrophobic layer over macroscopic distances [27]. Also, the tight-ion paired species formed with HCl by the complex $[(HR_2DTO)_2Pt]$ is capable to donate HCl to an amine. This capability has been successfully exploited for the spectrophotometric determination of aliphatic amines, given that the neutral complex and its HCl tight-ion paired species exhibit different absorptions in the visible region [28]. Moreover, in the solid state, the HCl tight-ion paired species exhibits photoluminescence, which is lost by heating or by exposing the sample to ammonia vapors [29].

In our previous review published in ICA [27] the role of ligands and of metal in affecting the factors which govern the properties as second order NLO chromophores of the following triads [M(Bz_2pipdt)(dmit)]; [M($^iPr_2$pipdt)(dmit); [M(Bn_2pipdt)(dcbdt)] (dcbdt = dicyanobenzodithiolato); [M(Bn_2pipdt)(mnt)] (mnt = maleonitrile-2,3-dithiolate) and [M(Et_2dazdt)(mnt)] (Et_2dazdt = N,N'diethyl-perhydrodiazepine-2,3-dithione) has been discussed. Structural, electrochemical, spectroscopic, and electric-field-induced second-harmonic generation (EFISH) measurements as well as density functional theory (DFT) and time-dependent-DFT (TD-DFT) including polarizable continuum method (PCM), have shown that the obtained high negative second-order polarizability values are related to the high difference in dipole moments between excited and ground state enhanced by the electric field of the solvent, the large oscillator strength for the CT transition, and the relatively low energy gap, in agreement with the two-state theoretical approximation (Fig. 1). Moreover, steric factors affecting the electronic distribution and thus the NLO properties, have been pointed out. It was concluded that the best candidate to maximize the second-order NLO activity among the investigated triads, results the one composed of Pt (II), R_2pipdt, and dmit, which exhibits the lowest torsion angle between the two thioamido groups of the dithionic ligand and the larger π-

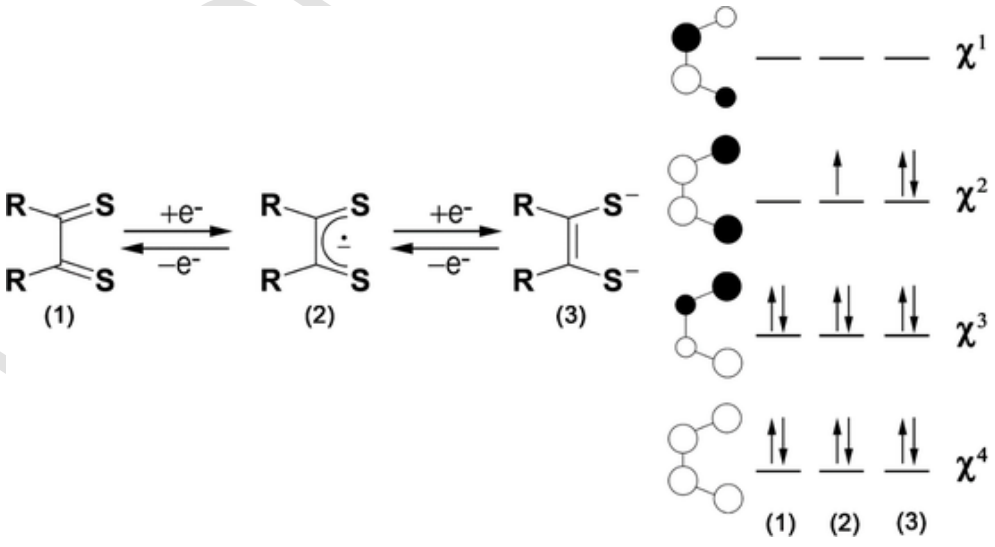

Scheme 1. On the left: redox processes involving α-dithione ligands. On the right: qualitative molecular orbital description.

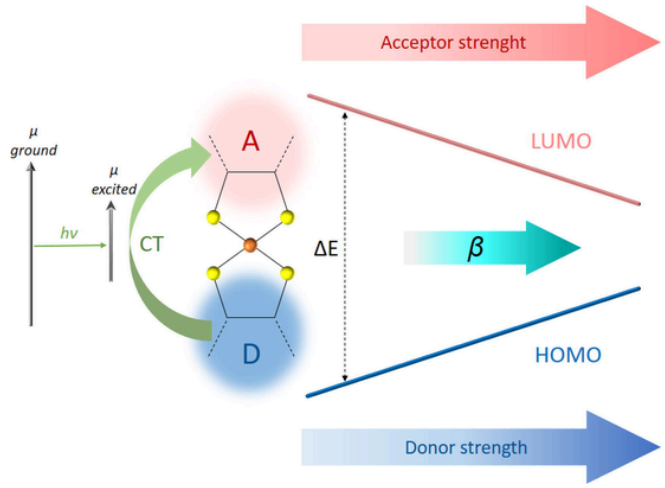

Fig. 1. Schematic representation of properties tunability in heteroleptic d^8 metal dithiolenes.

Chart 1.

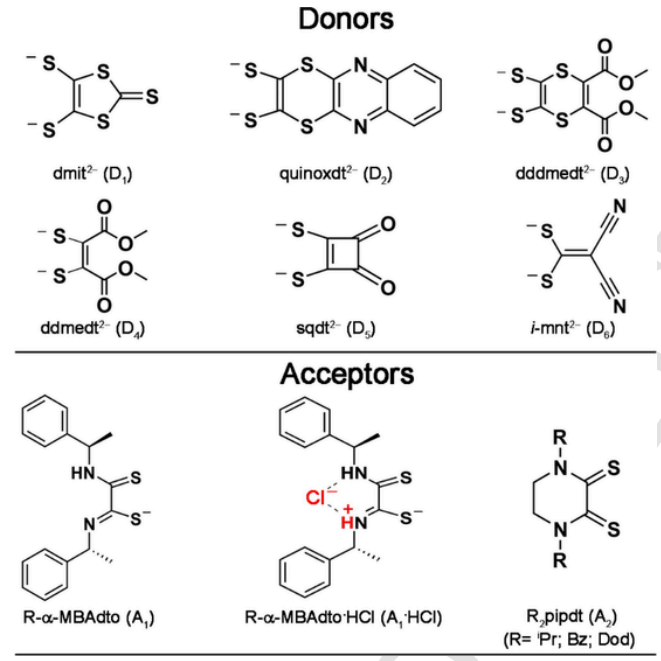

system extent of the dithiolato ligand, as shown in Fig. 2. The reversible bleaching of the solvatochromic peak on monoreduction of these Pd- and Pt-complexes, suggested their potential as switchable redox-active NLO-chromophores.

In this mini-review, the progress of our studies on this class of d^8metal-heteroleptic complexes, showing the capability of the novel derivatives to respond to external stimuli (protons, silver ions, and light-irradiation) to obtain multifunctional linear and nonlinear optical chromophores will be presented [31–35]. Promising and less promising results in the production of 2nd NLO-active materials where chromophores are embedded into polymeric PMMA (PolyMethylMethAcrylate) poled films or form crystals belonging to non-centrosymmetric point groups are also here shortly discussed.

2. Discussion

2.1. Second-order nonlinear response of d^8-metal heteroleptic dithiolenes

2.1.1. Solution 2nd NLO-proton switchable properties of complexes sharing the same dithiooxamidate Acceptor (R)-α-MBAdto.

The complexes **[MA$_1$D$_n$]$^-$** shown in Chart 2, have been obtained by combining the **D$_1$**, **D$_2$**, and **D$_4$** Donors with the Acceptor **A$_1$**.[32,36] The Donors, with approximately similar donating properties, are functionalized at the C2S2 moiety with a condensed heterocycle in **D$_1$**, with a thioether bridge connecting a quinoxaline ring in **D$_2$**, and two ester groups in **D$_4$**. The acceptor **A$_1$** presents homochiral stereo-centers suitable to promote the crystallization of the compounds in non-centrosymmetric space groups. Moreover, through its capability to undergo proton exchange, NLO switching in these D-M-A systems has been achieved. Structural data of **Bu$_4$N[MA$_1$D$_n$]** salts helped in elucidating the bonding in these complexes: the metals exhibit a square-planar geometry, with the M-S bond distances derived from the Donor ligand slightly shorter than those derived from the dithiooxamidate ligand. This is in agreement with the different charges of the two ligand systems, 2-for the dithiolato system and 1-for the dithiooxamidate system. The two SCN moieties of the dithiooxamidate system present bond distances that reflect monoprotonation of one N atom with the adjacent C—S fragment with a prevalent thione-nature, while the other C—S fragment exhibits a more pronounced thiolate feature.

In Table 1 the optical features of the chromophores **[MA$_1$D$_n$]$^-$** (M = Pd, Pt; n = 1, 2, 4) are summarized [36]. On HCl addition the λ_{max} of peaks related to the CT DA transition, undergo a shift to lower frequencies. On protonation, the negative $\mu\beta_\lambda$ values exhibit a remarkable increase by a factor ranging from 2.5 to 6.5, as a consequence of the increase of the Acceptor character of **A$_1$** following the formation of the tight-contact ion pair A1·HCl displayed in Fig. 3. The process can be reversed, and the $\mu\beta_\lambda$ values of the starting NLO-phores **[MA$_1$D$_n$]$^-$** are fully restored after NH_3 addition as shown for **[PtA$_1$D$_4$]$^-$** in Fig. 3 as an example. Thus, on changing the pH, efficient NLO switching is obtained. The $\mu\beta_\lambda$ values of the NLO-chromophores, as well as all those reported in this paper, have been determined by the EFISH technique working at the non-resonant 1907 nm incident wavelength. This technique allows obtaining more reliable data with respect the Hyper-Rayleigh Scattering technique, working at 1064 nm and commonly employed to study proton NLO switches in solution, since the possible overestimation of the value of the quadratic hyperpolarizability due to resonance can be prevented.

In addition, the modifications of the linear optical properties, described in the related section, make these complexes valuable multifunctional molecular switches which exhibit contrast in both nonlinear and linear optical properties which can be followed by the naked eyes.

2.1.2. Solution 2nd NLO properties of complexes sharing the same R_2pipdt Acceptor.

In Table 2 the optical features of complexes bearing R_2pipdt (**A$_2$**) as Acceptor are summarized. Inspection of Table 2 further confirms that inside the D-M-A systems, those based on **M**, **A$_2$** and **D$_1$** components exhibit the highest values of $\mu\beta_\lambda$, in the Pt-case the highest so far reported for metal complexes, to the best of our knowledge. These values are also higher than those of the corresponding **[MA$_2$D$_2$]** compounds, [32] despite both systems exhibit a similar HOMO-LUMO gap and related absorption maxima. The observed results can be explained considering the shape of the FOs involved in the CT transitions. In fact, the final states in the **D$_1$** case show a π-orbital system which also involves the periphery of the ligand, differently to the **D$_2$** corresponding orbitals, which are less extended because of the presence of the thio-ether bridges that confer a bended structure to the ligand. On the other side the bended structure of **D$_2$** has shown to be valuable in providing additional peculiar luminescent properties to the derived complexes, as

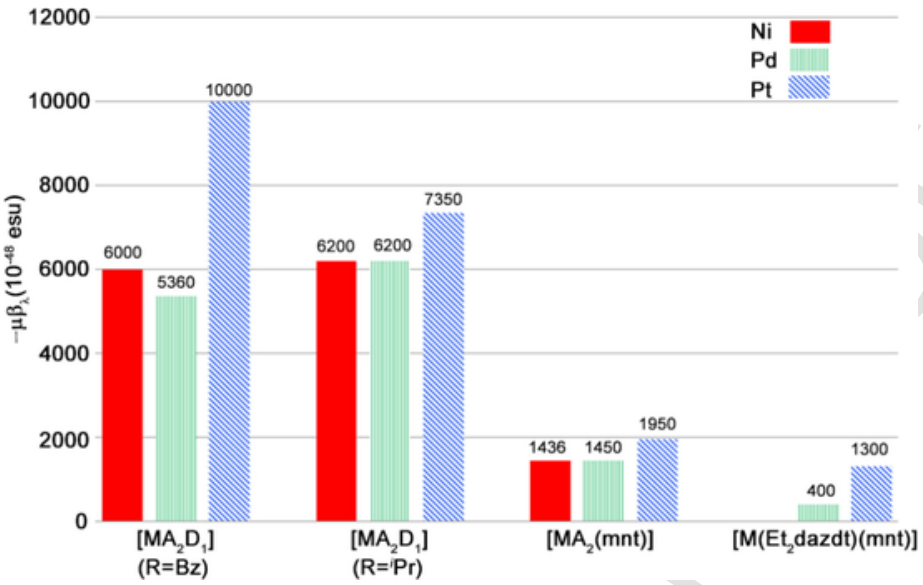

Fig. 2. $\mu\beta_\lambda$ values of d^8 metal dithione–dithiolato complexes triads on variation of the metal, the donor and the acceptor ligands.

Chart 2.

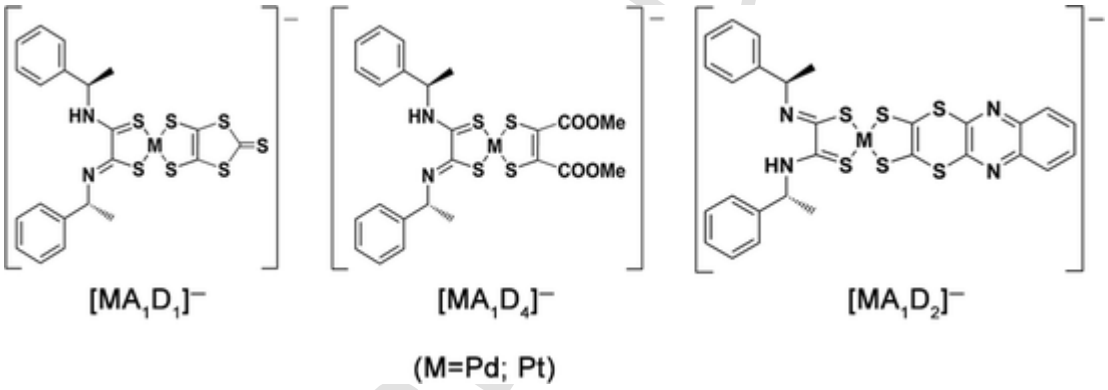

Table 1
Optical properties of **$[MA_1D_n]^-$** and related tight-ion paired complexes (ref. [36]).

	λ_{max}(nm)[a] [ε x10^3 (M^{-1} cm^{-1})]	$\mu\beta_\lambda$ [b]	$\mu\beta_\lambda$($[MA_1D_n]^-$·HCl)/$\mu\beta_\lambda$ ($[MA_1D_n]^-$)		λ_{max}(nm) [ε x10^3 (M^{-1} cm^{-1})]	$\mu\beta_\lambda$ [b]	Kurtz	PMMA film(pm V^{-1})
$[PdA_1D_1]^-$	525 [15.7][c]	−590	3.8	**$[PdA_1D_1]^-$·HCl**	747 [6.7]	−2210	≈ 0	5.34
$[PtA_1D_1]^-$	543 [9.6]***	−1020	2.5	**$[PtA_1D_1]^-$·HCl**	781 [9.6]	−2560	≈ 0	n. a.
$[PdA_1D_4]^-$	525 [4.0]	−390	5.7	**$[PdA_1D_4]^-$·HCl**	715 [5.7]	−2210	0.2	2.02
$[PtA_1D_4]^-$	558 [5.5]	−480	**6.5**	**$[PtA_1D_4]^-$·HCl**	764 [11.1]	−3120	0.5	1.32
$[PdA_1D_2]^-$	550 [5.5]	−615	3.2	**$[PdA_1D_2]^-$·HCl**	773 [5.8]	−1970	≈ 0	n. a.
$[PtA_1D_2]^-$	606 [6.7]	−735	4.0	**$[PtA_1D_2]^-$·HCl**	814 [12.4]	−2980	≈ 0	n. a.

[a] In DMF solutions. [b] **10^{-48} esu**. [c] These values include the contribution from a typical ligand absorption.

summarized in the related section, making them multi-responsive compounds.

As a last comment on the $\mu\beta_\lambda$ values on corresponding complexes where the central metal is changed (Table 1, Table 2), it can be once more pointed out that platinum derivatives exhibit the highest value inside the triads. This has been related to the highest metal contribution to the HOMO by the d_{xy} orbital of platinum with respect to that of the other metal centers, so favoring the extent of the π-orbital system and the oscillator strength, as reflected by the observed more intense CT bands [30].

The same **A_2** Acceptor (R = Bz) has been employed to synthesize Ni-complexes **$[NiA_2\text{-}D_n]$** (n = 3–6), on varying the Donor [33]. Despite, as said, the corresponding platinum-complexes would exhibit larger NLO responses, the use of nickel-metal offers advantages in terms of cost and depletion of precious metals as well as in terms of higher solubility of related complexes in common organic solvents. Thus, it

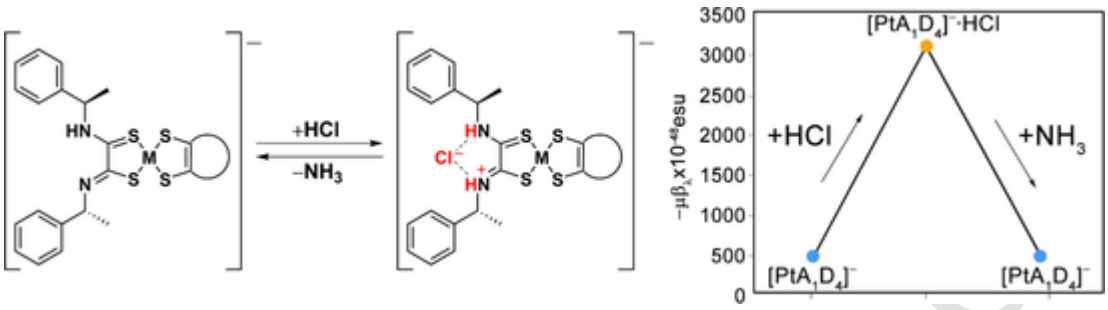

Fig. 3. Proton exchange equilibria for $[MA_1D_n]^-$ (n = 1, 2, 4) and on the right: the NLO proton switch with increase for $[PtA_1D_4]^-$ by a factor of 6.5.

Table 2
Optical properties of **[MA_2D_n]**.

	λ_{max}(nm)[f] [ε x10^3 (M^{-1} cm^{-1})]	$\mu\beta_\lambda$(10^{-48}) esu	PMMA film(pm V^{-1})
[NiA_2D_2] [a] R = ^{i}Pr	863 [8.0]	−1490	n. a.
[PdA_2D_2] [a] R = ^{i}Pr	773 [3.8]	−1970	n. a.
[PtA_2D_2] [a] R = ^{i}Pr	836 [10.5]	−4280	n. a.
[NiA_2D_3] [b] R = Bz	678 [6.5]	−680	≈ 0
[NiA_2D_4] [b] R = Bz	737 [7.4]	−855	≈ 0
[NiA_2D_5] [b] R = Bz	830 [6.1]	−1080	2.20
[NiA_2D_6] [b] R = Bz	872 [8.0]	−1180	≈ 0
[NiA_2D_1]			
R = Bz [c]	858 [10.6]	−6100	n. a.
R = ^{i}Pr [d]	827 [8.6]	−6200	n. a.
[PdA_2D_1]	819 [11.3]	−5360	n. a.
R = Bz [c]	775 [5.5]	−4700	n. a.
R = ^{i}Pr [d]	801 [4.4]	−2665	1.86
R = Dod [e]			
[PtA_2D_1]			
R = Bz [c]	827 [14.8]	−10000	n. a.
R = ^{i}Pr [d]	790 [13.3]	− 7300	n. a.

[a] ref. [29]; [b] ref. [30]; [c] ref. [36]; [d] ref. [37]; [e] ref. [38]; [f] In DMF solutions.

seemed preferable to us to start with nickel complexes to investigate the capability of these class of complexes to be embedded into a poled polymeric matrix to achieve NLO-response in the bulk (see related section). The obtained μβλ values determined in DMF solution for **[NiA_2-D_n]** complexes are still remarkable (Table 2), and their increase is relatable to the λ_{max} increase of the CT absorptions, in agreement with the calculated HOMO-LUMO gap, as shown in Fig. 4. Being mainly associated to the acceptor's orbitals, LUMOs energies of these complexes are very similar. Thus, the differences in the FOs gaps between these compounds are mostly related to the energy of the HOMOs.

On variation of the Acceptor (Table 1 and Table 2), complexes with the same metal and Donor, show a μβλ increase following the sequence **A_1 < A_1·HCl < A_2**, according to the increased Acceptor capability. As shown in Fig. 5 for D = **D_1**, the HOMOs energies of these complexes are very similar because they are mainly due to the Donor's orbitals, thus the differences in the FOs gaps between these compounds are mostly related to the energy of the LUMOs.

2.1.3. 2nd NLO response in the bulk.

To maintain the 2nd NLO-response in the bulk, the corona-wire poling technique on composite thin films of chromophores dispersed in a polymeric matrix is widely employed [3]. In this technique the starting isotropic material is ordered by the application of a large DC electric field while the material is heated to just below the glass transition temperature (T_g) of the polymeric matrix. This is done since the decrease of the viscosity of the matrix near the T_g, allows an easier orientation of the NLO chromophores. After the SHG signal reaches a plateau, the temperature is decreased to room temperature, "freezing" the orientation of the chromophores inside the polymeric matrix, and the electric field is turned off. During the cooling process and after the removal of the electric field, the SHG signal is monitored as a function of time and temperature, to check whether or not reorientation of the chromophores within the polymeric matrix occurs in the explored time and temperature range. This technique has been employed on thin films of **[NiA_2-Dn]** (A_2 = Bz_2pipdt, n = 3–6) [33] and of **Bu_4N[PdA_1D_1]**; **Bu_4N[PdA_1D_4]** and **Bu_4N[PtA_1D_4]** [35] dispersed in PMMA matrix.

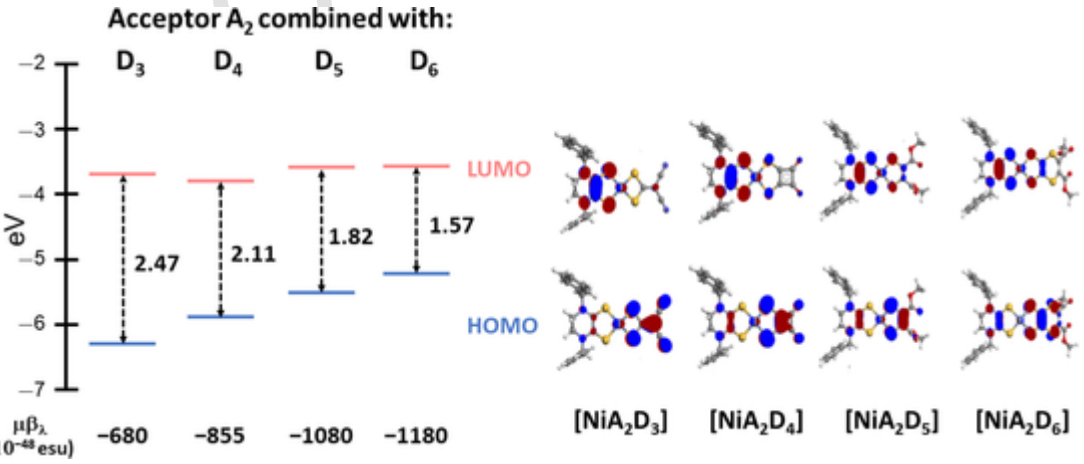

Fig. 4. Frontier molecular orbital for [NiA_2Dn]. The Energy gap decrease between the FOs is mainly due to the HOMO's energy level, and is in agreement with the experimentally observed trend in $\mu\beta_\lambda$ values.

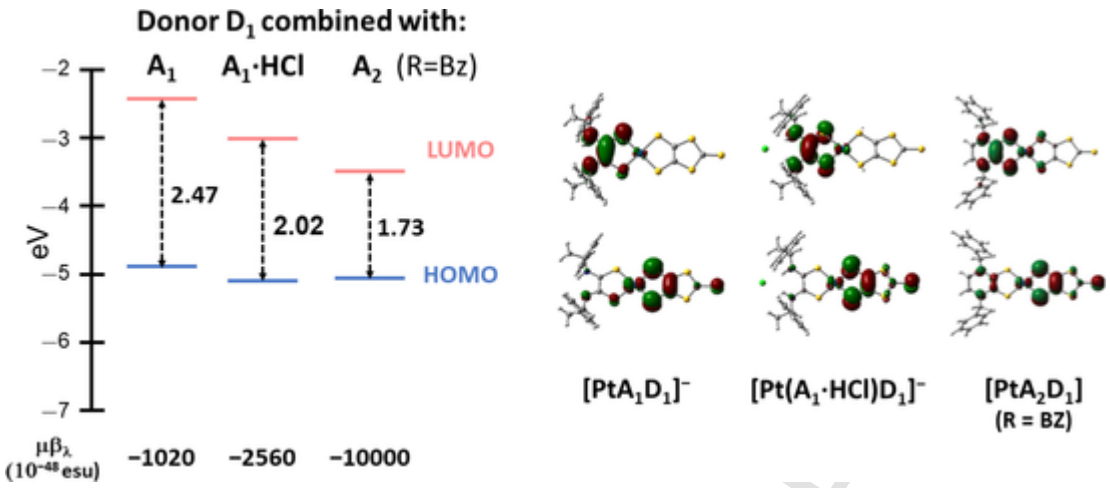

Fig. 5. Frontier molecular orbital for $[PtA_1D_1]^-$; $[Pt(A_1{\cdot}HCl)D_1]^-$; $[PtA_2D_1]$. The Energy gap decrease between the FOs is mainly due to the LUMO's energy level.

The SHG signals, negligible at room temperature, reach a maximum value as the temperature is increased around T_g of the PMMA and the electric field applied. During the cooling process only films of **[NiA$_1$D$_4$]** showed a stable SHG response ($\chi_{33}^{(2)}$ = 2.20 pm V^{-1}), while a fast decrease of the signal of the remaining Ni-based films was observed, despite all the samples exhibited similar thermolytic behaviour. The presence of ester groups attached to the dithiolate moiety in **D$_4$** seems to favour a suitable assembly of these NLO-phores in the polymer film to achieve a stable and good SHG response in the bulk. This seems supported by results on thin films of **Bu$_4$N [PdA$_1$D$_4$]** and embedded into PMMA ($\chi 33^{(2)}$ (**[PdA$_1$D$_4$]**$^-$) = 2.02 pm/V; $\chi^{33}{}^{(2)}$ (**[PtA$_1$D$_4$]**$^-$) = 1.32 pm/V) Fig. 6. A good and stable response ($\chi^{33(2)}$ = 5.34 pm/V) was also obtained with **Bu$_4$N [PdA$_1$D$_1$]** bearing dmit as Donor (see Table 1). These good SHG responses seem very promising [22 and related references therein available], however attempts to protonate the films with HCl vapors failed, probably due to the difficulty of the acid to penetrate into the polymeric PMMA matrix. Replacement of PMMA by different polymer will be pursued to try to obtain the desired goal.

The **Bu$_4$N [MA$_1$Dn]** (M = Pd, Pt; n = 1, 2, 4) salts, despite crystallizing in non-centrosymmetrical space group, as predictable for the presence of homochiral stereo-centers in (*R*)-α-MBAdto, did not show a measurable SHG response, determined according to the Kurtz-Perry method at 1907 nm on crystalline powders, except in the case of **Bu$_4$N [PtA$_1$D$_4$]** (0.5 by comparing intensity with the urea standard). These findings have been ascribed to the different arrangements of the chromophores in the crystals: those containing **D$_1$** and **D$_2$** as Donors crystallize in the non-polar $P2_12_12_1$ space group, which, despite being non-centrosymmetric, is one of the unfavorable space groups to allow for a non-null SGH signal. Instead the **Bu$_4$N [PtA$_1$D$_4$]** crystallizes in the polar *P*1 space group, and two independent complex molecules, with different orientations, are present in the asymmetric unit (see Fig. 7).

In concluding this section, it may be underlined that D-M-A complexes based on heteroleptic d^8-metal dithiolenes well illustrate how all the three components (D-M-A) play a role in affecting the NLO properties of a given complex and further confirm their versatility to control NLO responses by properly engineering the components both to optimize $\mu\beta_\lambda$ values and/or to obtain proton-switching. As far as SHG in the

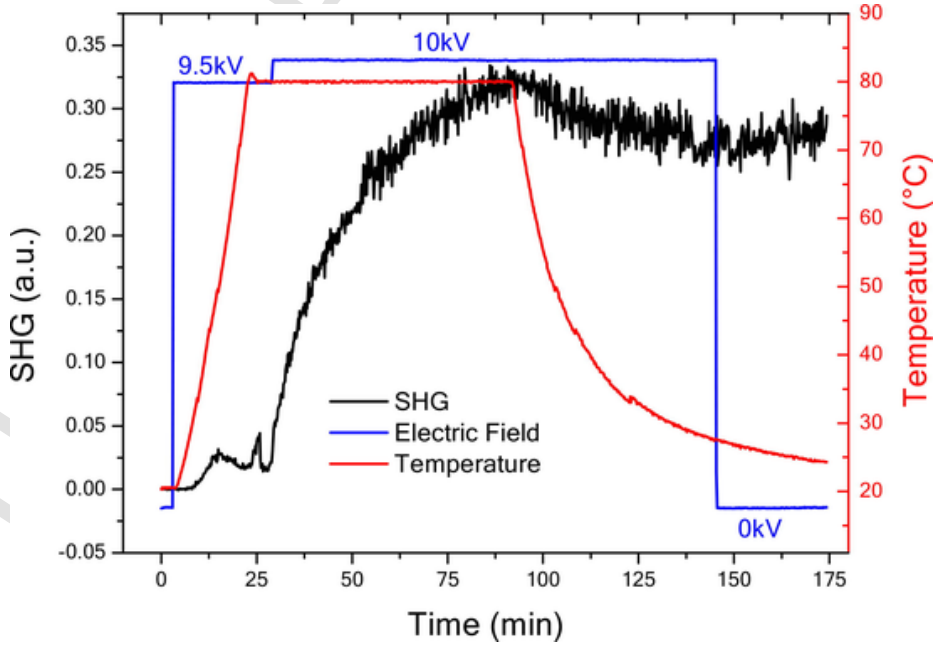

Fig. 6. Poling of the Bu$_4$N[PtA$_1$D$_4$] PMMA film. SHG (black line) temperature (red line) and electric field (blue line). (For interpretation of the references to color in this figure legend, the reader is referred to the web version of this article.)

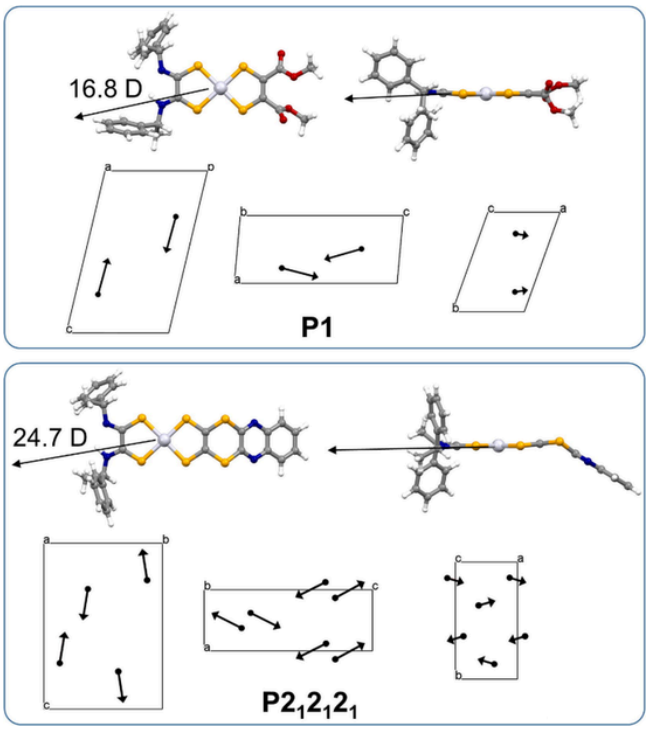

Fig. 7. DFT calculated dipole moment and orientation of the dipole moment within the unit cell of $[PtA_1D_4]^-$ (above) and $[PtA_1D_2]^-$ (below).

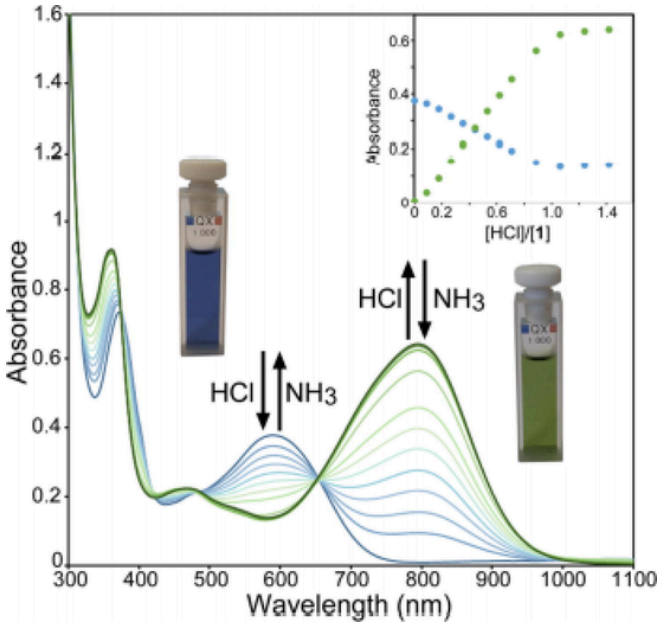

Fig. 8. Variation of the absorption upon successive additions of HCl (10 μL, 10^{-3} M) and NH_3 (10 μL, 10^{-3} M) to a solution of $[PtA_1D_2]^-$ in CH_3CN (1 mL, 1×10^{-4} M). In the inset, plots of the absorbance values at 588 nm (blue) and 795 nm (green) against [HCl]/[$Bu_4N[PtA_1D_2]$] are reported. Reprinted with permission from ref. [31]. Copyright 2021 American chemical Society. (For interpretation of the references to color in this figure legend, the reader is referred to the web version of this article.)

bulk is concerned, stable and large response was obtained for thin films in few cases. However, failure in protonating PMMA films of the proton switchable NLO-phores, suggests that alternative pathways (different polymeric matrices, or strategies) must be explored to overcome the difficulty of the acid to penetrate the polymeric PMMA matrix. Also, the poor SHG response of crystals clearly shows that further studies-strategies are required to achieve non-centrosymmetric crystals in suitable polar space groups.

2.2. Linear optical properties. Proton and silver switchable chromism

Table 1 includes absorptions assigned to the D-A CT transitions of the listed chromophores. The reversible protonation processes for **$Bu_4N[MA_1D_n]$** (M = Pd, Pt; n = 1, 2, 4) described in Section 2.2.1, is accompanied by a color change in accordance with the shift of the peak to higher wavelengths as shown in Fig. 8 for **$[PtA_1D_2]^-$** as an example.

Interestingly these complexes have shown to be capable to further interact with a different type of electrophile such as the silver ion. In this case the addition of silver trifluoromethanesulfonate (AgOTf) to **$Bu_4N[MA_1Dn]$** (M = Pd, Pt; n = 1, 2, 4) in DMF solutions is accompanied by the formation of a new peak at lower wavelengths. The presence of isosbestic points and the trend of absorbances at λ_{max} versus increasing AgOTf amounts allowed us to reasonably suggest the formation of a 1:2 adduct between the reagents. Removal of silver ions, for example upon HCl addition, allows the recovery of the protonated complexes as shown in Fig. 9 for **$[PtA_1D_2]^-$** as a representative example.

Computational studies by means of DFT methods taking into account the solvent with the PCM provided great support to elucidate the observed behaviour. In Fig. 10 the FOs of **$[PtA_1D_2]^-$** and of its AgOTf and HCl adducts are displayed as an example. As predictable, the HOMO is mainly localized on the dithiolate system, whereas the LUMO is mainly localized on the dithio-oxamidate fragment. The slightly non-symmetric shape of the HOMO and LUMO reflects the presence of a hydrogen atom on only one of the thioamido groups of the **A_1** ligand. A good agreement between the experimental and TD-DFT calculated visible spectra has been found, also confirming that the low energy absorption band is associated almost exclusively to an HOMO → LUMO transition. The HOMO → LUMO gap increases as a consequence of the HOMO stabilization on formation of the AgOTf adduct, while this gap decreases as a consequence of the LUMO stabilization on formation of the HCl adduct. In the HCl adduct the most favourable protonation site is the nitrogen atom of **A_1**, with a double N—H···Cl hydrogen bond formation and a consequent more symmetrical shape of the MOs which confers a significant stabilization to the LUMO. This is fully consistent with the observed shift of the low-frequency peak and related color changes.

2.2.1. Linear optical properties: Proton and silver switchable photoluminescent properties

Commonly d^8 metal heteroleptic dithiolene complexes do not exhibit luminescent properties, neither in solution at room temperature nor in glassy solvents at 77 K, with the exception of those containing the quinoxdt donor (**D_2**). It has been found that both the homoleptic radical **$[Pt(D_2)_2]^-$** [40] and heteroleptic **$[PtA_1D_2]^-$** [35] and **$[PtA_2D_2]$** [32] complexes are emissive in solution at room temperature and, remarkably, the observed emission falls above the energy of the lowest-energy absorption, pointing to an "anti-Kasha" behaviour [41,42] (*Kasha's Rule*: The emitting level of a given multiplicity is the lowest excited level of that multiplicity). The origin of this peculiar emissive behaviour is ascribed to the **D_2** ligand and in particular to the sequence and localization of the FOs as calculated from DFT and schematized in Fig. 11a. As it can be seen, the superior excited energy level corresponds to a MO (LUMO + 1) that is highly localized on the periphery of the **D_2** ligand. The poor spatial overlap with the LUMO, mainly associated to the dithiolene core, makes the direct (radiative) decay to the ground state (corresponding to the HOMO) kinetically competitive with respect to the commonly observed relaxation through nonradiative interconversion (IC) mechanism between adjacent energy levels. These considerations, together with the significant energy gap between the LUMO + 1 and the HOMO -related energy levels justify the observed radiative emission originating from an ILCT transition within the **D_2** lig-

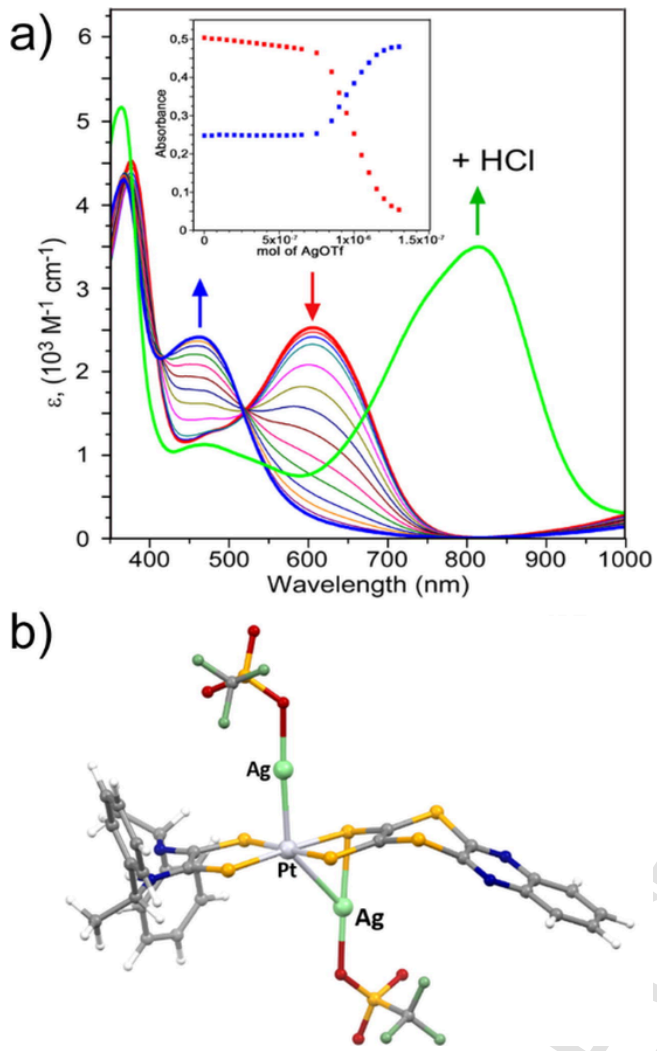

Fig. 9. a) UV-vis-NIR spectra of silver titration of $[PtA_1D_2]^-$ in DMF solution (concentration 1 × 10^{-4} M). (b) DFT optimized geometry of $[PtA_1D_2]$·2AgOTf: B3lyp/6–31 + G(d)_SDD with pseudopotentials on Pt (MWB60) and Ag (MWB28) with the PCM method (dimethylformamide). Adapted with permission from ref. [35]. Copyright 2021 American chemical Society.

and of unusual anti-Kasha character. The proposed mechanism has also been validated through advanced transient absorption studies which have allowed tracing back the evolution of the excited states of **$[PtA_1D_2]^-$** as representative compound [34]. These studies have highlighted the occurrence of an outstandingly long-lived excited state (1.4 ps in comparison to the typical sub-fs lifetimes of IC) compatible with an emission mechanism stemming from the second excited state.

Fig. 11b shows the steady-state photoluminescence (PL) spectra of the **D_2** ligand derivatives in DMF solution upon irradiation in the range 420–450 nm. As anticipated, photoexcitation is solely possible in a spectral region well above the lowest absorption band of the compounds falling in the visible region and typically corresponding to an HOMO-LUMO transition of LL'CT character (see diagram of Fig. 11a). Interestingly, while **$[Pt(D_2)_2]^-$** and **$[PtA_2D_2]$** show a similar emission spectrum peaked at ca. 570 nm and corresponding to a yellow emission, in **$[PtA_1D_2]^-$** the LUMO + 1 is stabilized resulting in a peculiar emission in the deep red region with a maximum at 715 nm. More importantly, all these systems show reversible stimuli-responsive luminescence responding to acid (HCl) (Fig. 11c) and silver triflate addition (Fig. 11d). Protonation on the nitrogen donor atoms of the quinoxaline ring (where the LUMO + 1 is mainly located) in **$[Pt(D_2)_2]^-$** causes a change of the distribution of the electron density resulting in the quenching of the emission. However, initial conditions can be fully restored on addition of ammonia. Similar considerations can be made for the behaviour of **$[PtA_2D_2]$** upon silver triflate addition (Fig. 11d), which quenches the emission as a consequence of the formation of an adduct involving an interaction between the silver ion and the sulphur atoms on the dithiolene core. This adduct formation affects the distribution of the electron density and the sequence of the MOs (in particular the LUMO and LUMO + 1, Fig. 12) providing an alternative excited state deactivation channel through the dσ* orbitals of Ag^+. In this case, reversibility of the system properties is obtained after the addition of stoichiometric amounts of HCl which sequestrates the Ag^+ ions from the adduct yielding the pristine complex. Contrary to the emission turn off observed in **$[Pt(D_2)_2]^-$** and **$[PtA_2D_2]$**, **$[PtA_1D_2]^-$** presents a remarkable luminescence colour switch both in the presence of HCl and silver triflate. As shown in Fig. 3, the dithioxamidate ligand **A_1** can accommodate the HCl molecule yielding a tight-ion paired species of the compound. As highlighted by DFT calculations, this interaction causes a destabilization of the LUMO + 1 leading to an increased energy gap with the upper energy levels and justifying the observed blue shift of the emission turning from deep red to yellow-green (λ_{max} = 570 nm, Fig. 11c). Once again, the addition of ammonia fully recovers the pristine compound. Similar considerations can be drawn for the interaction of **$[PtA_1D_2]^-$** with silver triflate, which, contrary to the above cited case of **$[PtA_2D_2]$**, leaves the MOs sequence unaltered after the formation of a 2:1 adduct, but induces and increment of the energy gap of the ground and emissive levels. This results in an emission colour shifting to orange (λ_{max} = 620 nm, Fig. 11d) which can be reversed to the original deep red on NH_3 or HCl addition. **$[PtA_1D_2]^-$** represents a quite unique example of a fully reversible "turn on" luminescence sensor which displays emission in three different spectral ranges upon response to diverse stimuli (Fig. 11e). This behaviour is realized thanks to the synergistic effect of the emissive **D_2** ligand and the capability of the chiral **A_1** ligand to interact with external analytes in specific modes. The analogous palladium complex displays similar properties, where the emission colour is modulated by the effect of the different metal ion involved. These results highlight the potential of these compounds for various applications in sensing.

3. Final remarks

This mini-review has been addressed to survey the progress of the studies on heteroleptic d^8-metal dithiolenes exhibiting linear and non-linear optical properties. The Donors (dithiolato) and Acceptors (dithioxamide and dithioxamidate) of interest in this review, exhibit different electronic and/or structural features, varying from rigid and planar systems to conformationally-flexible ones. The obtained complexes show large quadratic hyperpolarizability, tunable on tuning each of the D–M-A components. Each of these components contributes in modulating both the energy and topology of the frontier molecular orbitals that are involved in the D-A CT process mediated by the metal. D and A ligands, combined with platinum and capable to form an extended π-orbital system including metal *d*-orbitals, confirm to be the most suitable to provide a low HOMO-LUMO gap, an excited-state dipole moment lower from the ground-state one, a large oscillator strength, and consequently high values of the negative quadratic hyperpolarizability. Moreover, on widening the functionality of the D and A components, switchable non-linear and linear chromophores capable to respond to external stimuli (non-linear: proton-responsive; linear: proton and silver-responsive; light-irradiation) have been obtained. Worthy to note, D-M-A (D = **D_2** = quinoxdt and A = **A_1** = [(*R*)-*α*-MBAdtox]) complexes, in addition to proton switchable NLO-properties, show emissive properties that are unique inside this class of compounds. This is achieved thanks to the combined action of **A_1**, able to react with protons, and **D_2**, carrier of luminescent properties and capable to interact with silver ions. It can be remarked that the properties

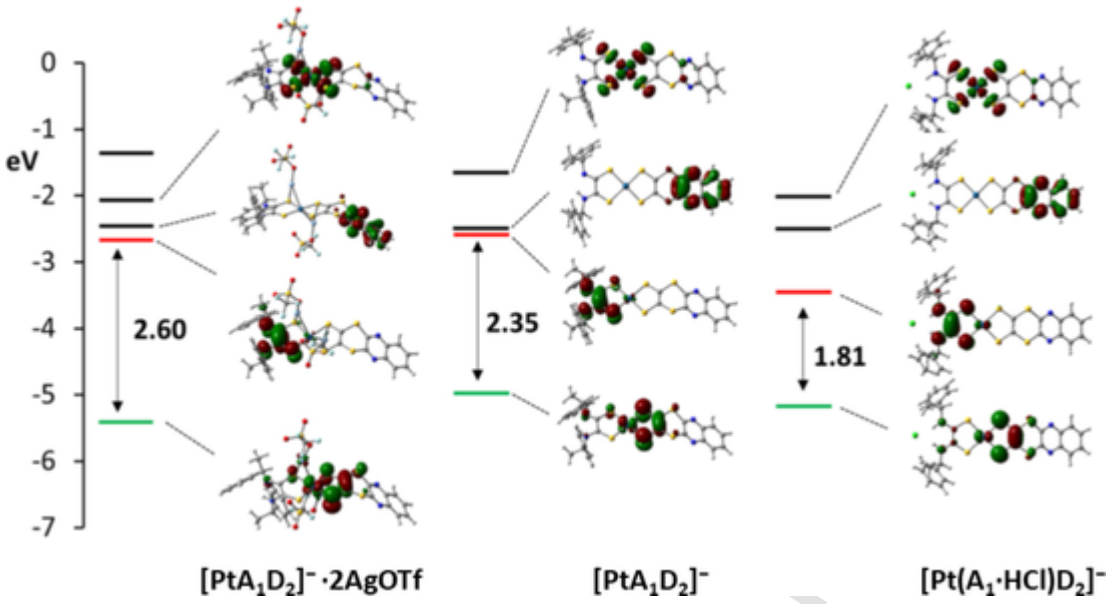

Fig. 10. Energy levels and Kohn-Sham MOs for the adducts $[PtA_1D_2]^{-}\cdot 2AgOTf$ (left), $[PtA_1D_2]^{-}$, and $[Pt(A_1\cdot HCl)D_2]^{-}$ (right). The calculations were performed at the B3LYP/6–31 + G(d)_SDD level with the PCM method in N,*N*-dimethylformamide. HOMO green bar, LUMO red bar, energy gap in eV. Reprinted with permission from ref. [35]. Copyright 2021 American chemical Society. (For interpretation of the references to color in this figure legend, the reader is referred to the web version of this article.)

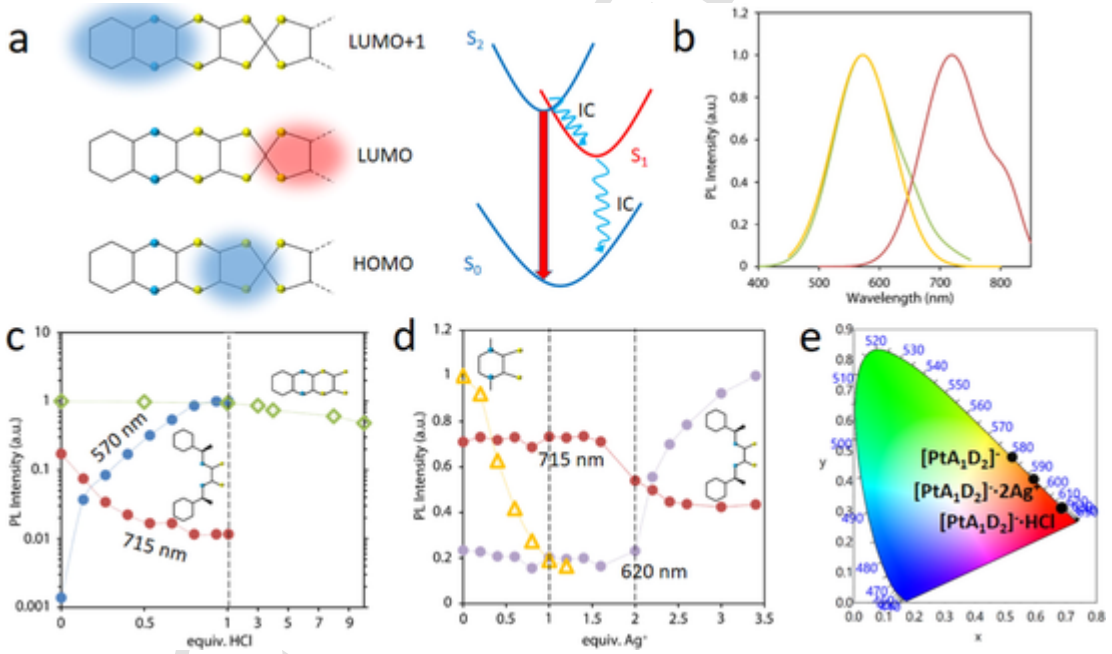

Fig. 11. a) General simplified scheme of the frontier MOs and mechanism of anti-Kasha-emission (red arrow) in platinum derivatives with the ligand D_2; b) normalized emission spectra of the heteroleptic $[PtA_1D_2]^{-}$ (red), $[PtA_2D_2]$ (yellow) and of the homoleptic radical $[Pt(D_2)_2]^{-}$ complexes (green) in DMF solution; c) PL emission intensity plotted on a logarithmic scale as a function of the equivalents of HCl added for $[PtA_1D_2]^{-}$ (circles) and $[Pt(D_2)_2]^{-}$ (diamonds).; d) PL emission intensity as a function of the equivalents of Ag^{+} added for $[PtA_1D_2]^{-}$ (circles) and $[PtA_2D_2]$ (triangles). Dashed lines are a guide to the eye. The insets show the structure of the ligands completing the Pt-D_2 backbone sketched in a). e) CIE1931 diagram reporting the emission colors of $[PtA_1D_2]^{-}$, its silver adduct $[[PtA_1D_2]^{-}\cdot 2AgOTf]$ and its tight-ion paired species with HCl $[([Pt(A_1\cdot HCl)D_2]^{-}]$. (For interpretation of the references to color in this figure legend, the reader is referred to the web version of this article.)

of these multi-responsive optical switches can be followed by the naked eye. Computational studies have shown to be useful to rationalize the experimental results and provide useful suggestions for future works to finely design the components to reach the desired properties. Attempts to transfer the NLO-properties in the bulk were successful for chromophores dispersed in PMMA films in a limited number of cases. As crystals, complexes bearing **A₁**, despite crystallizing in non-centrosymmetrical space groups for the presence of homochiral stereocenters in **A₁**, show a weak or not measurable SHG response. This is relatable to unfavourable orientation of molecules in the asymmetric unit. Reported achievements and failures are addressed to stimulate future work to exploit the potential of this class of complexes as linear and non-linear optical molecular sensors and switches and to optimize the processing procedures to achieve good SHG responses in the bulk.

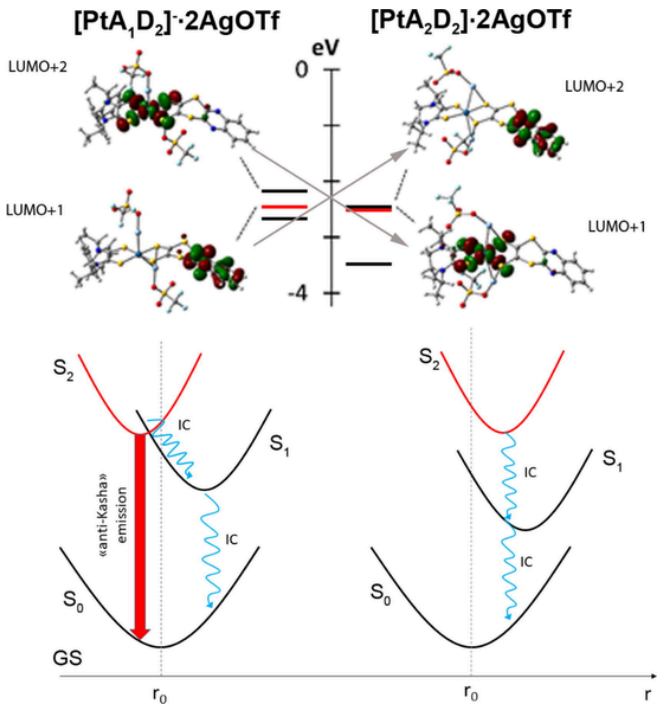

Fig. 12. Comparison of the virtual MOs (above) and simplified scheme of the relaxation from the second superior excited state (corresponding to the LUMO + 1) of $[PtA_1D_2]$·2AgOTf (left) and $[PtA_2D_2]$·2AgOTf·(right) (below). The LUMO + 1 is depicted in blue. r is the molecular coordinate and r_0 is the equilibrium coordinate of the ground state (taken as the HOMO). IC = internal relaxation. (For interpretation of the references to color in this figure legend, the reader is referred to the web version of this article.)

Uncited references

[13,14,15,16,17,18,19,20,21,39].

Declaration of Competing Interest

The authors declare that they have no known competing financial interests or personal relationships that could have appeared to influence the work reported in this paper.

Acknowledgements

The work of collaborators who have cooperated along the years to this topic are gratefully acknowledged. In particular to achieve the results reviewed here, the contributions of Dr Salahuddin S. Attar for the synthesis and characterization; of Prof. A. Cannizzo for the photoemissive properties; of Prof. M. Pizzotti and collaborators for the NLO-properties were crucial.

References

[1] R. W. Boyd, Nonlinear Optics, ed., Academic Press, New York, 1992, G.S. He (Ed.), Nonlinear Optics and Photonics, Oxford University Press, Oxford, 2015.
[2] P.N. Prasad, D.J. Williams, Introduction to Nonlinear Optical Effects in Molecules and Polymer, John Wiley & Sons, New York, 1991.
[3] L.R. Dalton, P.A. Sullivan, D.H. Bale, Electric Field Poled Organic Electro-optic Materials: State of the Art and Future Prospects, Chem. Rev. 110 (1) (2010) 25–55.
[4] G.G.A. Balavoine, J.-C. Daran, G. Iftime, P.G. Lacroix, E. Manoury, J.A. Delaire, I. Maltey-Fanton, K. Nakatani, S. Di Bella, Organometallics 18 (18) (1999) 21–29.
[5] M. Li, Y. Li, H. Zhang, S. Wang, Y. Ao, Z. Cui, Molecular engineering of organic chromophores and polymers for enhanced bulk second-order optical nonlinearity, J. Mater. Chem. C 5 (17) (2017) 4111–4122.
[6] D.R. Kanis, M.A. Ratner, T.J. Marks, Optical nonlinearities of conjugated molecules. Stilbene derivatives and highly polar aromatic compounds, Chem. Rev. 67 (1994) 195–242.
[7] J. Wu, B.A. Wilson, D.W. Smith Jr., S.O. Nielsen, Towards an understanding of structure/nonlinearity relationships in triarylamine-based push-pull electro-optic chromophores: the influence of substituent and molecular conformation on molecular hyperpolarizabilities, J. Mater. Chem. C 2 (2014) 2591–2599.
[8] P. Beaujean, F. Bondu, A. Plaquet, J. Garcia-Amoros, J. Cusido, F. M. Raymo, F. Castet, V. Rodriguez, B. Champagne, Oxazines: A New Class of Second-Order Nonlinear Optical Switches, J. Am. Chem. Soc. 138 (2016) 5052−5062.
[9] P. S. Marqués, J. M. A. Castàn, B. A. L. Raul, G. Londi, I. Ramirez, M. S. Pshenichnikov, D. Beljonne, K. Walzer, M. Blais, M. Allain, C. Cabanetos, P. Blanchard, Triphenylamine/Tetracyanobutadiene-Based π-Conjugated Push–Pull Molecules End-Capped with Arene Platforms: Synthesis, Photophysics, and Photovoltaic Response, Chem. Eur. J. 26 (2020) 16422 – 16433.
[10] T. Yanbe, K. Mizuguchi, R. Yamakado, S. Okada, Optical property control of p-electronic systems bearing Lewis pairs by ion coordination, Chem. Commun. 56 (2020) 10654–10657.
[11] B.J. Coe, Comprehensive Coordination Chemistry II, J.A. McCleverty, T.J. Meyer TJ Eds., Elsevier Pergamon Oxford, U.K., Nonlinear Optical Properties of Metal Complexes, 9 (2004) 621-687.
[12] S. Di Bella, C. Dragonetti, M. Pizzotti, D. Roberto, F. Tessore, R. Ugo, Topics in Organometallic Chemistry 28. Molecular Organometallic Materials for Optics, in: H. Le Bozec, V. and Guerchais (eds.), Springer Verlag Berlin Heidelberg 28 (2010), 1.
[13] D. Roberto, R. Ugo, F. Tessore, E. Lucenti, S. Quici, S. Vezza, P. Fantucci, I. Invernizzi, S. Bruni, I. Ledoux-Rak, J. Zyss, Effect of the Coordination to M(II) Metal Centers (M = Zn, Cd, Pt) on the Quadratic Hyperpolarizability of Various Substituted 5-X-1,10-phenanthrolines (X = Donor Group) and of trans-4-(Dimethylamino)-4'-stilbazole, Organometallics 21 (1) (2002) 161–170.
[14] F. Nisic, E. Cariati, A. Colombo, C. Dragonetti, S. Fantacci, E. Garoni, E. Lucenti, S. Righetto, D. Roberto, J.A. Gareth Williams, 'Tuning the dipolar second-order nonlinear optical properties of 5-π-delocalized-donor-1,3-di(2-pyridyl) benzenes, related cyclometallated platinum(II) complexes and methylated salts, Dalton Trans. 46 (2017) 1179–1185.
[15] G.D. Batema, M. Lutz, A.L. Spek, C.A. van Walree, G.P.M. van Klink, G. van Koten, Organometallic benzylidene anilines: donor–acceptor features in NCN-pincer Pt(II) complexes with a 4-(E)-[(4-R-phenyl)imino]methyl substituent, Dalton Trans. 43 (2014) 12200–12209.
[16] R. D'Amato, A. Furlani, M. Colapietro, G. Portalone, M. Casalboni, M. Falconieri, M.V. Russo, Synthesis, characterisation and optical properties of symmetrical and unsymmetrical Pt(II) and Pd(II) bis-acetylides. Crystal structure of trans-[Pt(PPh3)2(CC–C6H5)(CC–C6H4NO2)], J. Organomet. Chem. 627 (1) (2001) 13–22.
[17] Raphaël. J. Durand, Sébastien Gauthier, S. Achelle, S. Kahlal, J.-Y. Saillard, A. Barsella, L. Wojcik, N. Le Poul, F. Robin-Le Guen, Robin-Le Guen, Incorporation of a platinum center in the pi-conjugated core of push–pull chromophores for nonlinear optics (NLO), Dalton Trans. 46 (9) (2017) 3059–3069.
[18] S.D. Cummings, L.T. Cheng, R. Eisenberg, Metalloorganic Compounds for Nonlinear Optics: Molecular Hyperpolarizabilities of M(diimine)(dithiolate) Complexes (M = Pt, Pd, Ni), Chem. Mater. 9 (1997) 440–450.
[19] L. Pilia, M. Pizzotti, F. Tessore, N. Robertson, Nonlinear-optical properties of α-diiminedithiolato nickel(II) complexes enhanced by electron-withdrawing carboxyl groups, Inorg. Chem. 56 (2014) 4517–4526.
[20] G. Li, M.F. Mark, H. Lv, D.W. McCamant, R. Eisenberg, Rhodamine-Platinum Diimine Dithiolate Complex Dyads as Efficient and Robust Photosensitizers for Light-Driven Aqueous Proton Reduction to Hydrogen, J. Am. Chem. Soc. 140 (7) (2018) 2575–2586.
[21] L. Linfoot, P. Richardson, K.L. McCall, J.R. Durrant, A. Morandeira, N. Robertson, A nickel-complex sensitiser for dye-sensitised solar cells, Solar Energy 85 (2011) 1195–1200.
[22] A. Colombo, C. Dragonetti, V. Guerchais, D. Roberto, An excursion in the second-order nonlinear optical properties of platinum complexes, Coord. Chem. Rev. 446 (2021) 214113.
[23] Dithiolene Chemistry: Synthesis, Properties and Applications, Progress in Inorganic Chemistry, Vol.52, Special Vol. Ed. by E. I. Steifel, 2004 John Wiley& Sons, Inc, Hoboken, New Jersey.
[24] (a) S. Sproules, K. Wieghardt, Dithiolene radicals: Sulfur K-edge X-ray absorption spectroscopy and Harry's intuition. Coord. Chem. Rev. 255 (2011) 837–860. (b) P. Basu, K. J. Colston, B. Mogesa, Dithione, the antipodal redox partner of ene-1,2-dithiol ligands and their metal complexes. Coord. Chem. Rev. 409 (2020) 213211.
[25] J.L. Oudar, D.S. Chemla, Hyperpolarizabilities of the nitroanilines and their relations to the excited state dipole moment, J. Chem. Phys. 66 (1977) 2664–2668.
[26] J.L. Oudar, Optical nonlinearities of conjugated molecules. Stilbene derivatives and highly polar aromatic compounds, J. Chem. Phys. 67 (1977) 446–457.
[27] A. Giannetto, S. Lanza, F. Puntoriero, M. Cordaro, S. Campagna, Fast transport of HCl across a hydrophobic layer over macroscopic distances by using a Pt(II) compound as the transporter, Chem. Commun. 49 (2013) 7611–7613.
[28] A. Giannetto, M. Cordaro, S. Campagna, S. Lanza, Metal Complexes as Self-Indicating Titrants for Acid–Base Reactions in Chloroform, Inorg. Chem. 57 (2018) 2175–2183.
[29] F. Nastasi, F. Puntoriero, N. Palmeri, S. Cavallaro, S. Campagna, S. Lanza, Solid-state luminescence switching of platinum(II) dithiooxamide complexes in the presence of hydrogen halide and amine gases, Chem. Commun. 4740–4742 (2007).
[30] D. Espa, L. Pilia, S. Attar, A. Serpe, P. Deplano, Molecular engineering of heteroleptic metal-dithiolene complexes with optimized second-order NLO response, Inorg. Chimica Acta 470 (2018) 295–302.
[31] S.S. Attar, D. Espa, F. Artizzu, L. Pilia, A. Serpe, M. Pizzotti, G. Di Carlo, L. Marchiò, P. Deplano, Optically Multiresponsive Heteroleptic Platinum-dithiolene Complex with Proton Switchable Properties, Inorganic Chemistry 56 (2017) 6763–6767.

[32] S. S. Attar, F. Artizzu, L. Marchiò, D. Espa, L. Pilia, M. F. Casula, A. Serpe, M. Pizzotti, A. Orbelli Biroli, P. Deplano, Uncommon Optical Properties and Silver-responsive Turn-off/on Luminescence in a Pt(II) heteroleptic dithiolene complex, Chem. Eur. J. 24(2018) 10503-10512.
[33] S.S. Attar, L. Marchiò, L. Pilia, M.F. Casula, D. Espa, A. Serpe, M. Pizzotti, D. Marinotto, P. Deplano, Design of Nickel Donor-Acceptor Dithiolenes for 2nd order Nonlinear Optics. Experimental and Computational study, New J. Chem. 46 (2019) 12570–12579.
[34] M. Gazzetto, F. Artizzu, S. Attar, L. Marchio', L. Pilia, E. Rohwer, T. Feurer, P. Deplano, A. Cannizzo, Anti-Kasha Conformational Photo-isomerization of a Heteroleptic Dithiolene Metal Complex Revealed by Ultrafast Spectroscopy, J. Phys. Chem., Part A 124 (51) (2020) 10687–10693.
[35] S.S. Attar, L. Pilia, D. Espa, F. Artizzu, A. Serpe, M. Pizzotti, D. Marinotto, L. Marchiò, P. Deplano, An insight into the properties of heteroleptic metal dithiolenes: Multi-Stimuli Responsive Luminescence, Chromism and Nonlinear optics, Inorg. Chem. 60 (13) (2021) 9332–9344.
[36] D. Espa, L. Pilia, L. Marchio, M.L. Mercuri, A. Serpe, A. Barsella, A. Fort, S.J. Dalgleish, N. Robertson, P. Deplano, Redox Switchable Chromophores based on Metal (Ni, Pd, Pt) Mixed-Ligand Dithiolene Complexes Showing Molecular Second-order NLO Activity, Inorg. Chem. 50 (2011) 2058–2060.
[37] D. Espa, L. Pilia, L. Marchiò, S.S. Attar, A. Barsella, A. Fort, M.L. Mercuri, A. Serpe, Paola Deplano, Structural changes in MII dithione/dithiolato complexes (M = Ni, Pd, Pt) on varying the dithione functionalization, CrystEngComm 17 (2015) 4161–4171.
[38] D. Espa, L. Pilia, L. Marchiò, F. Artizzu, G. Di Carlo, D. Marinotto, A. Serpe, F. Tessore, P. Deplano, A nonlinear optical active polymer film based on Pd(II) dithione/dithiolate second-order NLO chromophores, Dalton Trans. 45 (2016) 17431–17438.
[39] D. Espa, L. Pilia, L. Marchiò, F. Artizzu, A. Serpe, M.L. Mercuri, D. Simão, M. Almeida, M. Pizzotti, F. Tessore, P. Deplano, Mixed-ligand Pt(II) dithione-dithiolato complexes: influence of the dicyanobenzodithiolato ligand on the second-order NLO properties, Dalton Trans. 41 (2012) 3485–3493.
[40] S. Attar, D. Espa, F. Artizzu, M.L. Mercuri, A. Serpe, E. Sessini, G. Concas, F. Congiu, L. Marchiò, P. Deplano, A platinum-dithiolene monoanionic salt exhibiting multi-properties, including room-temperature proton-dependent solution luminescence, Inorganic Chemistry 55 (2016) 5118–5126.
[41] L. Shi, C. Yan, Z. Guo, W. Chi, W. Liu, X. Liu, H. Tian, W.-H. Zhu, De novo strategy with engineering anti-Kasha/Kasha fluorophores enables reliable ratiometric quantification of biomolecules, Nat. Commun. 11 (2020) 793.
[42] H. Wang, J. Wang, T. Zhang, X. Zhang, H. Sun, Y. Xiao, T. Yu, W. Huang, Breaching Kasha's rule for dual emission: mechanisms, materials and applications, J. Mater. Chem. C 9 (2021) 10154–10172.